Self-Doped Polyaniline Nanoparticle Dispersions Based on Boronic Acid−Phosphate Complexation

Bhavana A. Deore and Michael S. Freund*

Department of Chemistry, University of Manitoba, Winnipeg, Manitoba R3T 2N2, Canada

Received September 5, 2008; Revised Manuscript Received November 17, 2008

ABSTRACT: Poly(anilineboronic acid)/phosphate nanoparticle dispersions are produced in high yields using the reactivity of the boronic acid moiety with phosphate in the presence of fluoride. The poly(anilineboronic acid)/phosphate dispersions have been characterized using spectroscopic, microscopic, and electrochemical techniques. According to ^{11}B NMR studies, the formation of anionic tetrahedral boronate group in phosphoric acid in the presence of fluoride forms the basis of self-doped, stabilized PABA nanoparticle dispersion. Transmission electron microscope images show that 25−50 nm diameter PABA nanoparticles are formed under these conditions. UV−vis, FT-IR-ATR spectroscopic, and cyclic voltammetric results confirm the formation of the conducting form of PABA. Films produced from these particles exhibit enhanced redox stability and potential dependent conductivity under neutral and basic pH conditions due to the formation of a boron−phosphate complex containing fluoride, which results in a self-doped form of the polymer.

Introduction

Conducting polymers exhibit semiconductor or metal-like electrical and optical properties while at the same time they are lightweight, flexible, inexpensive, and easy to synthesize.[1−3] However, the poor processability and stability of conducting polymers remains a key hurdle to their use in commercial applications. The limitations in postsynthesis processability are due to the chain stiffness and interchain interactions such as chemical or ionic cross-linking, rendering these materials insoluble in common solvents. In order to overcome these problems, several pre- and postsynthesis approaches have been developed including the reduction of polymer to nonconducting state, alkyl substitution, counterion-induced processability, enzyme synthesis, *in situ* polymerization of metastable monomer−oxidant mixtures, self-doping, and colloidal dispersions.[4] Recently, the restrictions on the use of organic solvents, due to environmental concerns, have encouraged the production of conducting polymers processable from aqueous media. In particular, colloidal dispersions and self-doped form of polyanilines (PANI) have been synthesized widely in aqueous media since they can be directly used in coatings,[5−7] molecular level processing,[8−11] lithography,[12,13] electrophoretic patterning,[14] and inkjet printing[15,16] for practical applications including chemical and biological sensors, antistatic coatings, corrosion protection, electrochromic devices, and energy storage. Stable dispersions of PANI colloidal particles are commonly obtained by chemical and electrochemical methods in the presence of surfactants and polymeric steric stabilizers.[17,18] During polymerization, steric stabilizers adsorb on the surface of growing PANI particles and prevent their aggregation and further macroscopic precipitation. For example, Wessling et al. have reported that PANI can be dispersed in water and different organic solvents by using counterions such as poly(styrenesulfonate), poly(methyl methacrylate), and *p*-toluenesulfonate.[19,20] Recently, Wang et al. prepared stable aqueous dispersions of PANI using phosphoric acid dopants with long and short hydrophilic ethylene glycol segments.[21,22]

In the present work, we report a new approach for synthesizing stable poly(anilineboronic acid) (PABA) dispersions in phosphoric acid using the complexation between the substituent boronic acid moiety on the PANI backbone and phosphate. Aromatic boronic acids are known to bind compounds containing diol moieties such as carbohydrates, vitamins, coenzymes, and ribonucleic acids[23] as well as fluoride[24,25] with high affinity through reversible ester formation. These interactions have been used to facilitate the chemical synthesis of water-soluble PABA under the polymerization conditions in the presence of sodium fluoride and excess D-fructose.[26] Self-doped PABA produced with this method has several advantages, including water solubility, good conductivity, and higher molecular weight. In addition, the intermolecular reaction between boronic acid groups and imines in PABA containing fluoride result in self-doped, self-cross-linked PABA with enhanced mechanical properties.[27] More recently, we have synthesized self-doped, alcohol-soluble PABA through boronic acid complexation with aliphatic alcohols and manipulated PABA morphology, i.e., nanostructures, with different shapes and forms through exchange of internal and external dopants.[28] Boron compounds such as borane, boric acid, and its ester are known to interact strongly with anions such as phosphate.[29,30] The binding of boron to phosphorus in boranophosphate compounds is reportedly air stable and has hydrolytic stability in both acid and base.[29] On the basis of these interactions, it was expected that water-soluble forms of PABA could be synthesized in the presence of phosphate.

Experimental Section

Materials. 3-Aminophenylboronic acid hydrochloride salt (3-APBA) and ammonium persulfate were purchased from Aldrich Chemical Inc. Sodium fluoride, potassium chloride, sodium phosphate, and phosphoric acid (85%) were purchased from Fisher Scientific. Bulk distilled water was filtered then ion exchanged to yield 18.2 MΩ·cm quality water using Milli-Q-Academic A10 (Millipore Corp.). Indium-doped tin oxide-coated glass slides (ITO, 6 ± 2 Ω/sq) were purchased from Delta Technologies Ltd. Gold interdigitated array microelectrodes (IDAs) were obtained from Biomedical Microsensors Laboratory at North Carolina State University. Each of these arrays contained 2.8 mm × 0.075 mm gold electrodes with a gap width of 20 μm that had a total exposed area of 0.069 mm^2. TEM Formvar-carbon coated copper grids (400 mesh) were purchased from CANEMCO-MARIVAC.

Synthesis of PABA/Phosphate Dispersions. PABA dispersions were synthesized using 10 mM (3-APBA) (monomer) and 50 mM sodium fluoride in 0.1 M phosphoric acid (20 mL) by adding 5 mM ammonium persulfate (oxidizing agent). Polymerization of 3-APBA was not observed in the absence of fluoride. A minimum

* Corresponding author. E-mail: michael_freund@umanitoba.ca.

10.1021/ma8020344 CCC: $40.75
Published on Web 12/11/2008

of 1 mol equiv of fluoride to monomer was required to obtain conducting PABA with >50% yields. The mixture was stirred at room temperature, and the reaction was allowed to proceed for 16 h. In phosphoric acid, PABA was well suspended under the polymerization conditions. As a result, PABA was isolated via centrifugation and subsequently purified (to remove excess reactants and byproducts) using 0.1 M phosphoric acid. Finally, the polymer was redispersed in 0.1 M phosphoric acid without fluoride. The dispersion of PABA nanostructures prepared in 0.1 M phosphoric acid is stable indefinitely (no settling was observed over a 2 month period) with a maximum concentration of 5 mg/mL. PABA dispersions can be prepared in concentrations up to 20 mg/mL; however, they do not remain suspended indefinitely. The dispersion of nanostructures was coated on gold IDAs and ITO electrodes for electrochemical and spectroscopic characterization.

Characterization. The morphology of the PABA dispersion was examined by transmission electron microscopy (TEM, JEOL JEM-2000FX). TEM samples were prepared by diluting the purified product and casting the dispersion onto copper grids. UV−vis absorption spectra of PABA dispersions were obtained using an Agilent 8453 spectrophotometer. Fourier transform infrared (FT-IR) spectra were obtained using a Nexus 870 spectrometer (Thermo Nicolet Corp.) equipped with an attenuated total reflectance (ATR) accessory. FTIR-ATR spectra of dry PABA powders were collected using a hemispherical germanium optical crystal and a deuterated triglycine sulfate and thermoelectrically cooled (DTGS TEC) detector. 32 interferograms were accumulated to obtain each FTIR-ATR spectrum at a spectral resolution of 8 cm^{-1}. Cyclic voltammetric and potential dependence drain current (I_D-V_G characteristic) measurements were performed using a CH Instrument CHI 760 electrochemical workstation. For both measurements, a three-electrode configuration was used including a Pt wire counter electrode, Ag/AgCl as a reference electrode, and gold IDA as a working electrode. The potentials were scanned from negative to positive directions. I_D-V_G characteristics were obtained by cycling the potential of the two adjacent PABA-coated microelectrodes (connected to W1 and W2 working electrode terminals of the bipotentiostat) maintaining a 50 mV potential difference between them. ^{11}B NMR studies were carried out using a Bruker AMX 500 NMR spectrometer. The samples were prepared by adding 10% D_2O in the monomer and polymer solution in 0.1 M phosphoric acid. Chemical shifts were determined relative to borontrifluoride etherate as a reference. X-ray photoelectron spectroscopic (XPS) analyses were carried out using Kratos Axis Ultra spectrometer with a base pressure of 2×10^{-10} mbar (UHV). A monochromatized Al Kα radiation source ($h\nu = 1486.70$ eV) was used. The X-ray electron gun was operated at 15 kV and 20 mA. The kinetic energy of the photoelectrons was analyzed in a multichannel delay-line detector (DLD).[31] Survey and high-resolution spectra were collected using 160 and 40 eV pass energies, respectively. The analyzed area of the samples was 700×300 μm^2. Spectra were acquired with electron charge compensation in operation to avoid sample charging. The binding energy scale was referenced to the C 1s peak of PABA, which was set to 284.6 eV. Core peaks were analyzed using a nonlinear Shirley-type background, and peak positions and areas were obtained by weighted least-squares fitting of model curves (70% Gaussian, 30% Lorentzian) to the experimental data. On the basis of the best practice of fitting the data for PABA, the maximum values of the fwhm were assigned for every single element, which were maintained equal during the component fit. The positions of component peaks were optimized to give the best fit to the experimental spectrum. The surface elemental compositions were determined by the ratios of peak areas corrected with sensitivity provided by Kratos for the Axis Ultra analyzer.[32]

Results and Discussion

The polymerization of 3-APBA in the presence of fluoride and phosphoric acid results in a stable PABA dispersion. In our previous studies, PABA dispersions consisting of 2−15 nm particle sizes were obtained using 0.1 M HCl and fluoride; however, they only remained suspended for 1 day.[28] In contrast, the larger size PABA particle dispersions prepared in the presence of phosphoric acid and fluoride are stable indefinitely; no settling was observed over a 2 month period at a concentration of 5 mg/mL. These results suggest that the stability of the dispersions in phosphoric acid relative to hydrochloric acid is due to the interaction of the phosphate with the boronic acid substituent.

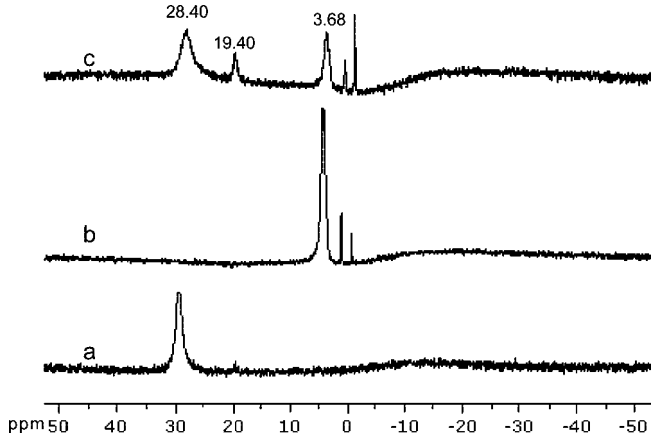

Figure 1. ^{11}B NMR spectra of monomer solution (a) 10 mM 3-APBA in 0.1 M phosphoric acid, (b) 10 mM 3-APBA + 50 mM NaF in 0.1 M phosphoric acid, and (c) polymer dispersion prepared using 10 mM 3-APBA + 50 mM NaF + 5 mM of ammonium persulfate in 0.1 M phosphoric acid and purified using 0.1 M phosphoric acid.

Table 1. N 1s Composition and Boron to Dopant Ratios in PABA/Phosphate Film Prepared from Dispersion

% N	71
% N^+	29
B:N	1:1
B:F	1:0.4
B:P	1:2

In order to explore this chemistry in more detail, an XPS study was performed on PABA film prepared from dispersions and rinsed with water. PABA dispersion was prepared in 0.1 M phosphoric acid and fluoride, and then it was purified and redispersed in the 0.1 M phosphoric acid without fluoride. The percentages of neutral nitrogen, positively charged nitrogen, B:F and B:P ratios in the PABA film are shown in Table 1. The neutral nitrogen is the sum of the two lowest binding energy components within the N 1s envelope and are attributed to the quinoid imine (−N=, ∼398.1 eV) and benzenoid amine (−NH−, ∼399.5 eV). The doping level of the polymer can be determined quantitatively based on the amount of dopant and the positively charged nitrogen (N^+, >400 eV) by deconvoluting the N 1s core-level spectrum.[33,34] Generally, in externally doped PANI with HCl, H_2SO_4, etc., the percentages of dopant and positively charged nitrogen are approximately same.[33,34] In PABA, the percentage of fluoride dopant is approximately the same as the positively charged nitrogen; however, the percentage of phosphate is in excess (see Table 1). These results suggest that the PABA prepared in the presence of phosphoric acid and fluoride involves the complexation of boron to phosphate and fluoride. On the basis of the B:P ratio, all borons in polymer are bound to two phosphate groups. However, the fluoride is associated with ∼40% of the total polymer.

The chemical structure of PABA was further studied with ^{11}B NMR by examining of both monomer and polymer solutions in phosphoric acid as shown in Figure 1. The chemical shift of the ^{11}B NMR signal of boronic acids is dependent on the hybridization state of the boron atom (trigonal versus tetrahedral). The ^{11}B NMR spectrum of the monomer in phosphoric acid (Figure 1a) shows a single resonance with a chemical shift of 28.8 ppm, indicating that boron exists primarily in the neutral

Scheme 1. Proposed Mechanism of 3-APBA−Phosphate Complexation and Polymerization

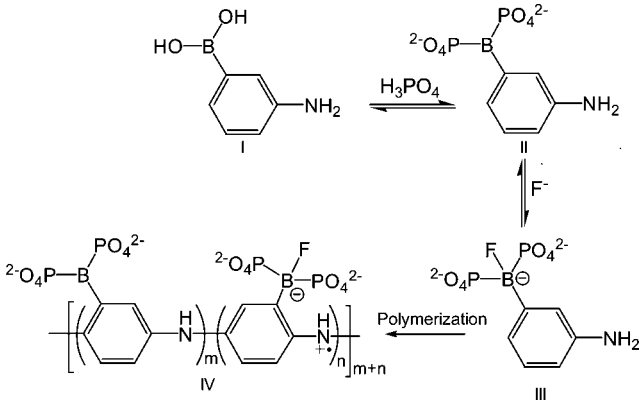

trigonal form (Scheme 1, II).[35] However, in the presence of sodium fluoride (Figure 1b), a resonance signal is observed ~25 ppm upfield, indicative of the formation of tetrahedral anionic boronate (Scheme 1, III).[24,25] Following the addition of an oxidizing agent, completion of the polymerization reaction, purification, and redispersion in 0.1 M phosphoric acid without fluoride, the ^{11}B NMR spectrum was taken again (Figure 1c). The spectrum shows that the boron exists in both trigonal boronic acid and tetrahedral anionic boronate form (Scheme 1, IV). The amount of tetrahedral boronate is ~35%. These results suggest that in monomer solution fluoride stabilizes tetrahedral boron (Scheme 1, III), which in turn allows oxidation of the monomer. Once the polymer is formed and oxidized, the oxidized backbone stabilizes the boron−phosphate complexation. The existence of multiple peaks in the PABA nanoparticle dispersion suggests that there are both tetrahedral and trigonal forms of boron which do not interconvert on the NMR time scale[36,37] as indicated by the peaks at 3.68 and 28.40, respectively, as well as some fraction of boron groups which experience fast interconversion, resulting in an averaged peak position[36,37] of 19.40 ppm. The percentage of tetrahedral boronate is in agreement with the percentage of positively charged nitrogen obtained from XPS study and suggests that the PABA is self-doped in phosphoric acid in the presence of fluoride and self-stabilized likely due to the formation of boron−phosphate complex. On the basis of both XPS and ^{11}B NMR results, the structure of self-doped PABA is composed of around 40% *n* and 60% *m* repeat units as shown in Scheme 1, IV. PABA/phosphate dispersions were prepared by varying monomer to oxidant ratios from 1:0.25 to 1:2. The stability of PABA particle dispersion with time as well as the redox conductivity as a function of pH was found to be higher at monomer to oxidant ratios of 1:0.5 due to the higher degree of self-doping at the optimum polymerization rate.

Figure 2 presents the TEM image of a PABA dispersion prepared in 0.1 M phosphoric acid and fluoride. The PABA dispersion was purified and redispersed in the 0.1 M phosphoric acid without fluoride. The morphology of PABA prepared in 0.1 M phosphoric acid and fluoride is somewhat similar to that obtained in 0.1 M HCl and fluoride. In 0.1 M HCl solution and fluoride, spherical nanoparticles with diameter in the range of 2−15 nm are obtained.[28] However, phosphate doped and complexed PABA produces irregular shape particles with size range 25−50 nm (Figure 2). The difference observed in the size and shape of PABA prepared in phosphoric acid can be attributed to the boron−phosphate complexation.

The FTIR-ATR spectrum of PABA/phosphate nanostructures depicts all of the characteristic bands of PANI and boron−phosphate interactions as shown in Figure 3, solid line. IR bands characteristic of PANI are observed at 1609, 1488, and 1140 cm^{-1} corresponding to quinoid, benzenoid, and the aromatic C−N stretching ring modes.[38] The characteristic bands of the B−F stretching modes are observed at 810, 850, and 882 cm^{-1}.[39] However, the asymmetric B−O stretching mode generally observed at 1340 cm^{-1} in boronic acids, as shown in Figure 3, dashed line, is not present in PABA/phosphate. Bands characteristic of phosphate are observed at 920, 980, 1077, 1232, and 1308 cm^{-1}.[39] The appearance of a sharp peak at 1572 cm^{-1} is attributed to the B−N dative bond.[40,41] However, this peak is not observed for PABA synthesized chemically without phosphate (Figure 3, dashed line).[27,42] Therefore, the presence of the peak at 1572 cm^{-1} and the absence of B−O stretching mode further supports that the other interactions such as boron−phosphate likely contribute to this peak, as shown in Scheme 1, IV.

The above spectroscopic results confirm the boron−phosphate interaction and formation of self-doped PABA. To further explore the role of phosphate, optical, electrochemical, and *in situ* conductivity properties of PABA as a function of pH have been studied. Figure 4 shows the UV−vis spectra of PABA dispersion as a function of pH. PABA dispersed in 0.1 M phosphoric acid resulted in a pH of 1, and the pH of the dispersion was subsequently increased by titrating with 1 M NaOH. The characteristic absorption bands around 320 and 800

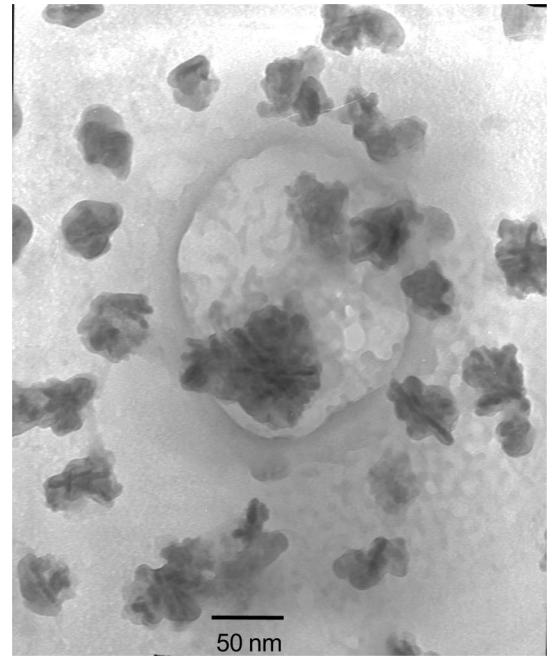

Figure 2. TEM micrograph of PABA/phosphate particles.

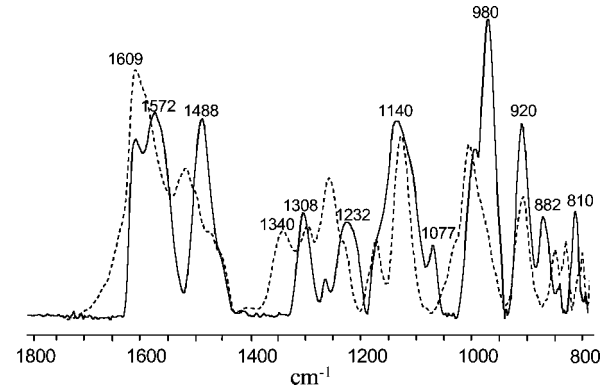

Figure 3. FTIR-ATR spectrum of PABA/phosphate dried powder (solid line) and PABA prepared chemically using 0.5 M HCl in the presence of fluoride (dashed line).

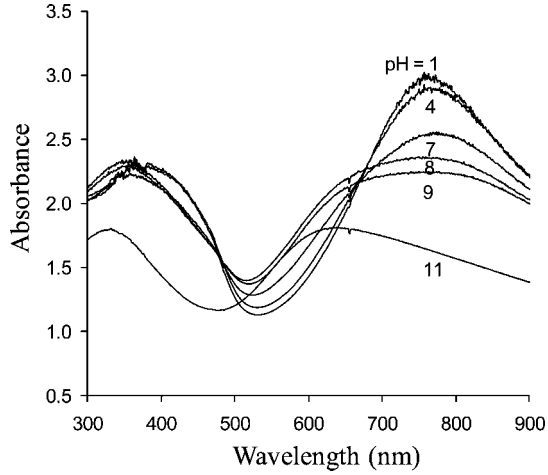

Figure 4. UV−vis spectra of PABA/phosphate dispersion as a function of pH.

nm assigned to $\pi-\pi^*$ and bipolaron band transitions, respectively, are observed up to pH 7.[43,44] The existence of these bands in the PABA dispersion indicates that the polymer is in the conducting emeraldine salt state up to pH 7. At pH values 8 and 9, the bipolaron band remained at 700−800 nm; however, it broadens and exhibits a slight blue shift. At a pH value of 11, the presence of a broad peak at 620 nm suggests the complete dedoping of PABA to the emeraldine base form of the polymer. The PABA dispersion was stable and remained green up to pH 9. Above pH 9, the nanoparticles undergo a color change from green to blue, consistent with dedoping as well as flocculation. The flocculation of nanoparticles results in a decrease in absorbance at pH 11 due to scattering. The dedoping of polymer obtained upon exposure to alkaline pH is likely due to removal of phosphate and fluoride and conversion from emeraldine salt to the base form.[26] In order to verify these results, the stability of PABA dispersion in pH 7.4 phosphate buffer with and without NaCl was examined as a function of time (Figure 5). The conversion of the dispersion from emeraldine salt to the base form of PABA is observed at pH 7.4 in the presence of phosphate buffered saline (containing NaCl) solution as shown in Figure 5A. In contrast, the PABA dispersion is highly stable in pH 7.4 phosphate buffered solution (in the absence of NaCl) as a function time (Figure 5B). These results suggest that boron forms an anionic tetrahedral boronate group in the presence of phosphate and fluoride, resulting in self-doping, and imparts conductivity stability of PABA dispersion as a function of pH. The exchange of phosphate with other anions such as chloride or hydroxide results in the dedoping of the PABA dispersion.

Figure 6 shows the pH-dependent redox and *in situ* conductivity behavior of a PABA dispersion coated onto an IDA. The cyclic voltammograms of PABA in the pH range 1−8 shown in Figure 6A suggest that PABA is redox active at neutral and above neutral pH. The oxidation and reductions peaks are dependent upon the pH of electrolyte solution. At pH 1−3, the presence of two sets of redox peaks is attributed to the facile conversion between oxidation states similar to unsubstituted PANI[45] and previously reported for chemically and electrochemically prepared PABA under acidic conditions in the presence of fluoride.[26,46,47] However, above pH 3, only one set of redox peaks is observed, suggesting that the emeraldine form is not stable in this pH range and that PABA is directly converted from the fully reduced leucoemeraldine to highly oxidized pernigraniline form. This pH-dependent redox behavior is consistent with self-doped PABA in the presence of D-fructose,[48] sulfonated self-doped PANI,[49] and PANI doped with

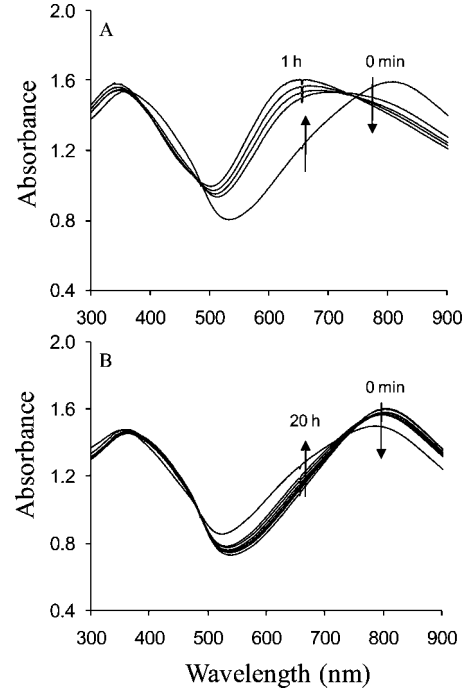

Figure 5. UV−vis spectra of PABA/phosphate in (A) phosphate buffered saline (with NaCl) and (B) phosphate solution (without NaCl) at pH 7.4 as a function of time.

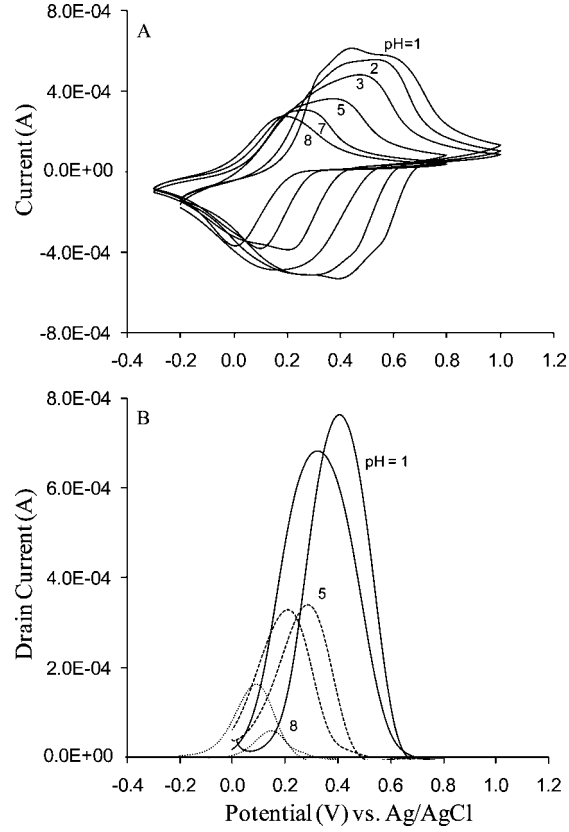

Figure 6. Cyclic voltammograms at 100 mV/s (A) and I_D-V_G characteristics at 5 mV/s (B) of PABA/phosphate coated IDA's as a function of pH of solution. The electrolyte pH solutions in the range of 1−8 are prepared using 0.5 M phosphoric acid and sodium bihydrogen phosphate.

phosphoric acid with long and short hydrophilic ethylene glycol segment.[22] Similar to these reports, the magnitude of peak current decreases as a function of pH of solution. However, the

decrease in current observed for PABA in the pH range of 1−8 is far less than the reported one order decrease for sulfonated self-doped PANI[49] and the two order decrease for PANI doped with phosphoric acid with long and short hydrophilic ethylene glycol segment.[22] The cyclic voltammograms of PABA are reproducible and reversible in the pH range 1−8. These results suggest that self-doped PABA, involving an anionic tetrahedral boronate in the presence of phosphate and fluoride, is stable even in the absence of fluoride in electrolyte solution and during cycling and thus extending the electroactivity of PABA to neutral and above neutral pH.

Figure 6B shows the I_D-V_G characteristic of PABA in a potential range 0.0−0.8 V as a function of solution pH. Throughout the entire pH range, I_D-V_G characteristics of PABA are reproducible from scan to scan. The I_D-V_G characteristics show that the potential window of high conductivity is pH dependent similar to the redox behavior. Also, the width of conducting region is narrowed from 0.6 to 0.4 V for pH 1−8. The conductivity was calculated from the ohmic current flowing through the film via two working electrodes using the formula $\sigma = i_\Omega/EA$ S/cm, where i_Ω is the ohmic current, E is the voltage offset between the electrodes divided by the distance between them, and A is the total effective cross-sectional area between the two arrays of electrodes.[50] The cross-sectional area is determined by the thickness of the film (0.3 μm) and their total length (7.84 cm), leading to $A = 2.35 \times 10^{-4}$ cm^2. The thickness of the film was calculated using the mass of the PABA, density, and electrode area. The measured spacing between the electrodes was 20 μm and the offset voltage between the electrodes of 50 mV. The conductivity of PABA reaches a maximum at a potential intermediate between the two states of being insulating fully reduced leucoemeraldine and fully oxidized pernigraniline form. At pH 1, the maximum conductivity of PABA is 0.14 S/cm at 0.4 V. The conductivity value decreased to 0.07 S/cm at 0.25 V and 0.03 S/cm at 0.1 V for pH 5 and 8, respectively. However, in the case of PANI, the reported maximum conductivity decreases almost 2 orders of magnitude from pH 0 to 4.[51]

Conclusions

The PABA dispersions prepared in phosphoric acid in the presence of fluoride involves boron−phosphate interactions and formation of an anionic tetrahedral boronate group, which forms the basis of self-doped PABA. The highly conducting PABA dispersion with 25−50 nm size particles can be prepared without using surfactants or stabilizers as a template. Because of self-doping, PABA dispersions have high electroactive and conducting stability in neutral and above neutral pH conditions. As a result, this material is an excellent candidate for pH, CO_2, and biosensors as well as for formulations for coatings and inkjet printing.

Acknowledgment. This work was supported by Natural Sciences and Engineering Research Council (NSERC) of Canada, the Canada Foundation for Innovation (CFI), the Manitoba Research and Innovation Fund, and the University of Manitoba. This research was undertaken, in part, thanks to funding from the Canada Research Chairs Program. We thank Dr. Kirk Marat for assistance with the NMR experiments and Dr. Sergei Rudenja for assistance with the XPS measurements.

Supporting Information Available: XPS data of PABA/phosphate film. This material is available free of charge via the Internet at http://pubs.acs.org.

References and Notes

(1) Shirakawa, H. *Angew. Chem., Int. Ed.* **2001**, *40*, 2575.
(2) Heeger, A. J. *Angew. Chem., Int. Ed.* **2001**, *40*, 2591.
(3) MacDiarmid, A. G. *Angew. Chem., Int. Ed.* **2001**, *40*, 2581.
(4) For example see references in: Freund, M. S.; Deore, B. A. *Self-Doped Conducting Polymers*; John Wiley & Sons, Ltd.: New York, 2007.
(5) Shimizu, S.; Saitoh, T.; Uzawa, M.; Yano, K.; Maruyama, T.; Watanabe, K. *Synth. Met.* **1997**, *85*, 1337.
(6) Jang, J.; Ha, J.; Kim, K. *Thin Solid Films* **2008**, *516*, 3152.
(7) Konagaya, S.; Abe, K.; Ishihara, H. *Plast., Rubber Compos.* **2002**, *31*, 201.
(8) Li, W.; Hooks, D. E.; Chiarelli, P.; Jiang, Y.; Xu, H.; Wang, H. *Langmuir* **2003**, *19*, 4639.
(9) Li, C.; Mitamura, K.; Imae, T. *Macromolecules* **2003**, *36*, 9957.
(10) Cao, T.; Wei, L.; Yang, S.; Zhang, M.; Huang, C.; Cao, W. *Langmuir* **2002**, *18*, 750.
(11) Kitty, K. Y.; Wong, H. L.; Chan, W. K.; Kwong, C. Y.; Djuristic, A. B. *Chem. Mater.* **2004**, *16*, 365.
(12) Angelopoulos, M.; Patel, N.; Shaw, J. M.; Labianca, N. C.; Rishton, S. A. *J. Vac. Sci. Technol.* **1993**, *11*, 2794.
(13) Hong, S.; Zhu, J.; Mirkin, C. A. *Langmuir* **1999**, *15*, 7897.
(14) Li, G.; Martinez, C.; Semancik, S. *J. Am. Chem. Soc.* **2005**, *127*, 4903.
(15) Jang, J.; Ha, J.; Cho, J. *Adv. Mater.* **2007**, *19*, 1772.
(16) Crowley, K.; OMalley, E.; Morrin, A.; Smyth, M. R.; Killard, A. J. *Analyst* **2008**, *133*, 391.
(17) Gangopadhyay, R.; De, A. *Chem. Mater.* **2000**, *12*, 608.
(18) Jang, J. *Adv. Polym. Sci.* **2006**, *199*, 189.
(19) Wessling, B. *Synth. Met.* **2003**, *135*, 265.
(20) Kahol, P. K.; Ho, J. C.; Chen, Y. Y.; Wang, C. R.; Neeleshwar, S.; Tsai, C. B.; Wessling, B. *Synth. Met.* **2005**, *151*, 65.
(21) Geng, Y. H.; Sun, Z. C.; Li, J.; Jing, X. B.; Wang, X. H.; Wang, F. S. *Polymer* **1999**, *40*, 5723.
(22) Luo, J.; Zhang, H.; Wang, X.; Li, J.; Wang, F. *Macromolecules* **2007**, *40*, 8132.
(23) For a review, see: (a) Springsteen, G.; Wang, B. *Tetrahedron* **2002**, *58*, 5291. (b) Springsteen, G.; Wang, B. *Tetrahedron* **2004**, *60*, 11205.
(24) Westmark, P. R.; Valencia, L. S.; Smith, B. D. *J. Chromatogr., A* **1994**, *664*, 123.
(25) Cooper, C. R.; Spencer, N.; James, T. D. *Chem. Commun.* **1998**, 1365.
(26) Deore, B. A.; Yu, I.; Freund, M. S. *J. Am. Chem. Soc.* **2004**, *126*, 52.
(27) Deore, B. A.; Yu, I.; Aguiar, P. M.; Recksiedler, C.; Kroeker, S.; Freund, M. S. *Chem. Mater.* **2005**, *17*, 3803.
(28) Deore, B. A.; Yu, I.; Woodmass, J.; Freund, M. S. *Macromol. Chem. Phys.* **2008**, *209*, 1094.
(29) Sood, A.; Shaw, B. R.; Spielvogel, B. F. *J. Am. Chem. Soc.* **1990**, *112*, 9000.
(30) Kameta, N.; Hiratani, K. *Chem. Lett.* **2006**, *35*, 536.
(31) Briggs, D.; Grant, J. T. *Surface Analysis by Auger and X-ray Photoelectron Spectroscopy*; IM Publication: Chichester, UK, 2003; p 138.
(32) Clarke, D. R.; Suresh, S.; Ward, I. M. *Surface Analysis of Polymers by XPS and Static SIMS*; Cambridge University Press: New York, 1998; p 44.
(33) Neoh, K. G.; Kang, E. T.; Tan, K. L. *J. Phys. Chem.* **1991**, *95*, 10151.
(34) Kang, E. T.; Neoh, K. G.; Tan, K. L. *Prog. Polym. Sci.* **1998**, *23*, 277.
(35) Domaille, P. J.; Druliner, J. D.; Grosser, L. W., Jr.; Schmelzer, E. R.; Stevens, W. R. *J. Org. Chem.* **1985**, *50*, 189.
(36) Kim, D. H.; Marbois, B. N.; Faull, K. F.; Eckhert, C. D. *J. Mass Spectrom.* **2003**, *38*, 632.
(37) Kim, D. H.; Faull, K. F.; Norris, A. J.; Eckhert, C. D. *J. Mass Spectrom.* **2004**, *39*, 743.
(38) Epstein, A. J.; McCall, R. P.; Ginder, J. M.; MacDiarmid, A. G. In *Spectroscopy of Advanced Materials*; John Wiley & Sons: New York, 1991.
(39) Socrates, G. *Infrared Characteristic Group Frequencies*, 2nd ed.; John Wiley & Sons: New York, 1994.
(40) Colthup, N. B.; Daly, L. H.; Wiberley, S. E. *Introduction to Infrared and Raman Spectroscopy*; Academic Press: New York, 1975.
(41) Chen, X.; Liang, G.; Whitmire, D.; Bowen, J. P. *J. Phys. Org. Chem.* **1998**, *11*, 378.
(42) Recksiedler, C.; Deore, B. A.; Freund, M. S. *Langmuir* **2005**, *21*, 3670.
(43) Stafstrom, S.; Breda, J. L.; Epstein, A. J.; Woo, H. S.; Tanner, D. B.; Huang, W. S.; MacDiarmid, A. G. *Phys. Rev. Lett.* **1987**, *59*, 1464.
(44) Wudl, F.; Angus, R. O.; Lu, F. L.; Allemand, P. M.; Vachon, D. J.; Nowak, M.; Liu, Z. X.; Heeger, A. J. *J. Am. Chem. Soc.* **1987**, *109*, 3677.
(45) Huang, W. S.; Humphrey, B. D.; MacDiarmid, A. G. *J. Chem. Soc., Faraday Trans.* **1986**, *82*, 2385.
(46) Nicolas, M.; Fabre, B.; Marchand, G.; Simonet, J. *Eur. J. Org. Chem.* **2000**, *9*, 1703.
(47) Deore, B. A.; Freund, M. S. *Analyst* **2003**, *128*, 803.
(48) Deore, B. A.; Hachey, S.; Freund, M. S. *Chem. Mater.* **2004**, *16*, 1427.
(49) Lukachova, L. V.; Shkerin, E. A.; Puganova, E. A.; Karyakina, E. E.; kiseleva, S. G.; Orlove, A. V.; Karpacheva, G. P.; Karyakin, A. A. *J. Electroanal. Chem.* **2003**, *544*, 59.
(50) Chidsey, C. E. D.; Murray, R. W. *J. Phys. Chem.* **1986**, *90*, 1479.
(51) Zhang, C.; Yao, B.; Huang, J.; Zhou, X. *J. Electroanal. Chem.* **1997**, *440*, 35.

MA8020344